EPJ manuscript No.
(will be inserted by the editor)

From Leading Hadron Suppression to Jet Quenching at RHIC and at the LHC

Urs Achim Wiedemann

Department of Physics, CERN, Theory Division, CH-1211 Geneva 23

Received: date / Revised version: date

Abstract. In nucleus-nucleus collisions at the Relativistic Heavy Ion Collider (RHIC), one generically observes a strong medium-induced suppression of high-p_T hadron production. This suppression is accounted for in models which assume a significant medium-induced radiative energy loss of high-p_T parent partons produced in the collision. How can we further test the microscopic dynamics conjectured to underly this abundant high-p_T phenomenon? What can we learn about the dynamics of parton fragmentation, and what can we learn about the properties of the medium which modifies it ? Given that inelastic parton scattering is expected to be the dominant source of partonic equilibration processes, can we use hard processes as an experimentally well-controlled window into QCD non-equilibrium dynamics ? Here I review what has been achieved so far, and which novel opportunities open up with higher luminosity at RHIC, and with the wider kinematical range accessible soon at the LHC.

PACS. 12.38.Mh – 24.85.+p

1 Introduction

High-p_T partons, propagating through the dense and spatially extended QCD matter created in a nucleus-nucleus collision, are expected [1,2,3,4,5,6,7,8] to suffer a significant medium-induced energy degradation prior to hadronization in the vacuum. Similar to electric charges propagating through QED matter, inelastic radiative contributions dominate over elastic collisional ones [1,9] for highly energetic projectiles. However, compared to its abelian analogue, radiative QCD energy loss shows characteristic differences which can be traced back to its non-abelian nature. In contrast to QED photon radiation, the gluonic quanta radiated off the hard projectile are color charged, and their interaction with the medium is even stronger than that of the parent projectile. This implies a significant p_T-broadening of the radiated remnants, and an approximately quadratic dependence of parton energy loss on in-medium path length.

The second qualitative difference between QCD parton energy loss and standard electrodynamic energy loss processes is that typical high-p_T partons are of high virtuality, $Q^2 \sim p_T^2$. Even in the absence of a nuclear environment, the uncertainty principle dictates that these partons must reduce their virtuality quickly on time (length) scales which turn out to be comparable to a nuclear diameter. They do so by breaking up into remnants of reduced virtuality. In the vacuum, this perturbative fragmentation process is described by an angular ordered DGLAP parton shower which has a probabilistic interpretation, and which underlies analytical approaches and Monte Carlo simulations of parton fragmentation. In the presence of a medium, there is an interference pattern between this "vacuum radiation" and the medium-induced radiation [6]. As a consequence, the leading parton (and a fortiori the leading hadron) in the shower emerges with reduced energy, the associated multiplicity of the jet is increased and softened, and the shower becomes broader.

Models based on this picture [10,11,12,13,14,15,16] account for the main modifications of high-p_T hadron production in nucleus-nucleus collisions at RHIC, namely the strong suppression of single inclusive hadron spectra, their centrality dependence [17,18,19,20,21,22], the corresponding suppression of leading back-to-back correlations [23], and high-p_T hadron production with respect to the reaction plane [24]. The above picture of the microscopic dynamics of medium-induced parton energy loss also makes predictions for two classes of measurements which are now gradually coming into experimental reach [25], namely i) high-p_T particle correlations [26,27], jet shapes and jet multiplicity distributions [28,29,30,31] which test the predicted relation between the energy loss of the leading parton, the transverse momentum broadening of the parton shower, and the softening of its multiplicity distribution and ii) the relative yields of identified high-p_T hadrons which test the prediction that medium-induced parton energy loss depends on the color charge and mass of the parent parton.

In my view, the main challenge for jet physics in nuclear collisions remains to gain a better understanding of the relation between the observed medium modifications, the partonic nature of equilibration processes and

the properties of the produced matter [25]. Progress in this direction is most likely to occur via a detailed testing of the microscopic dynamics of parton energy loss in a close interplay of theory and experiment. This is made possible by two basic properties of hard hadronic probes: they are *abundant* and they are *strongly sensitive* to medium effects. Their sensitivity ensures that the experimentally measured medium-effects are larger than the estimated theoretical and experimental uncertainties, and their abundant rates allow us to quantify more and more differential properties. Both features are prerequisits for a detailed characterization of the medium-modified partonic fragmentation pattern. This talk aims at emphasizing that such a detailed characterization is not *l'art pour l'art*, but provides one of the most promising approaches to learn about QCD equilibrium and non-equilibrium physics.

2 Current theory of parton energy loss

Parton propagation in a medium can be characterized by solving the Dirac equation for the corresponding partonic wave function in the color field of the medium [32,33]. In the limit of high projectile energy, the resulting S-matrix of any incoming parton is given by an eikonal path-ordered Wilson line

$$W(\mathbf{x}) = \mathcal{P} \exp\left[i \int dx^- A_a^+(\mathbf{x}, z^-)\, T^a \right] . \qquad (1)$$

Here, T^a is the $SU(3)$ generator in the representation of the propagating parton. The transverse coordinate $\mathbf{x}$ of the parton is frozen during propagation, but the parton rotates in color space due to the interaction with the target color field A_a^+ characterizing the medium. In general, production cross sections measure the extent to which different virtual components of the incoming partonic wavefunction pick up different phases and decohere during the scattering [34]. The target average of two fundamental Wilson lines at different transverse coordinates,

$$N(\mathbf{x}, \mathbf{y}) = 1 - \langle \mathbf{Tr}\, [W(\mathbf{x})\, W(\mathbf{y})] \rangle / N_c \,, \qquad (2)$$

is the simplest medium-dependent quantity which measures this phase decoherence. The high-energy limit of a large class of processes, including diffractive processes[32], gluon production in proton-nucleus collisions [35,34] and the photoabsorption cross section in the limit of small Bjorken x [33,34], have been formulated such that the target average (2) provides the entire information about the nuclear target.

In the study of medium-induced parton energy loss, we seek the multiple scattering-induced modifications of the bremsstrahlung gluon spectrum

$$dI^{\rm vac} = C_{F,A} \frac{\alpha_s}{\pi} \frac{dk_\perp^2}{k_\perp^2} \frac{d\omega}{\omega} \,. \qquad (3)$$

The total gluon bremsstrahlung spectrum is of the form

$$\omega \frac{dI^{\rm tot}}{d\omega\, d\mathbf{k}_\perp} = \omega \frac{dI^{\rm vac}}{d\omega\, d\mathbf{k}_\perp} + \omega \frac{dI^{\rm med}}{d\omega\, d\mathbf{k}_\perp} \,, \qquad (4)$$

where the medium modifications are power-suppressed, but parametrically larger than other power-suppressed corrections due to geometrical enhancements proportional to the large nuclear size. The distance between the production point of the hard parton in space-time and the typical position of a secondary scattering introduces a microscopic length scale (mean free path) relevant for the interference between vacuum and medium-induced radiation. To account for that, one has to go beyond the eikonal approximation by including the leading transverse Brownian motion of the produced partons. One finds that the medium-induced modification of (3) depends on the medium via the path-integral [5,6]

$$\mathcal{K}(\mathbf{r}_1, z_1; \mathbf{r}_2, z_2) = \int_{\mathbf{r}(z_1)}^{\mathbf{r}(z_2)} \mathcal{D}\mathbf{r} \exp\left[\int_{z_1}^{z_2} d\xi \left[i \frac{\omega}{2} \dot{\mathbf{r}}^2 - \frac{1}{2} n(\xi) \sigma(\mathbf{r}) \right] \right] , \qquad (5)$$

where

$$e^{-\frac{1}{2} n(\xi) \sigma(\mathbf{r})} \equiv \left\langle e^{i A_a^+(\mathbf{x}, \xi)\, T^a} e^{-i A_b^+(\mathbf{x}+\mathbf{r}, \xi)\, T^b} \right\rangle . \qquad (6)$$

In the limit of large gluon energy ω, the path integral (5) approaches the eikonal limit (2) of the target average of two Wilson lines. The expressions (2) and (6) encode essentially the same physical information, namely the transverse color field strength which the target presents to the hard partonic projectile. In (6), this information is parametrized in terms of a longitudinal density $n(\xi)$ times a measure of the transverse field strength per unit path-length, $\sigma(\mathbf{r})$. In terms of this target average, the medium-modification (4) of the gluon bremsstrahlung spectrum to leading order in parton energy and for arbitrarily large target color field reads [6,36]

$$\omega \frac{dI^{\rm med}}{d\omega\, d\mathbf{k}_\perp} = \frac{\alpha_s\, C_R}{(2\pi)^2\, \omega^2}\, 2{\rm Re} \int_{\xi_0}^{\infty} dy_l \int_{y_l}^{\infty} d\bar{y}_l \int d\mathbf{u}\, e^{-i \mathbf{k}_\perp \cdot \mathbf{u}} \times e^{-\frac{1}{2} \int_{\bar{y}_l}^{\infty} d\xi\, n(\xi)\, \sigma(\mathbf{u})} \frac{\partial}{\partial \mathbf{y}} \cdot \frac{\partial}{\partial \mathbf{u}} \mathcal{K}(\mathbf{y} = 0, y_l, \mathbf{u}, \bar{y}_l) \qquad (7)$$

For numerical applications, one approach is the opacity expansion of (7) which amounts to expanding the integrand in powers of the density $n(\xi)$ [6,7]. Alternatively, one exploits that the main support of the integrand of (7) is for small transverse distances which permits the harmonic oscillator approximation of the path integral with [5,4,6]

$$n(\xi)\, \sigma(\mathbf{r}) \approx \frac{1}{2} \hat{q}(\xi)\, \mathbf{r}^2 \,. \qquad (8)$$

Here, $\hat{q}$ is the so-called BDMPS transport coefficient which parametrizes the small distance behavior of the expectation value of the gauge invariant operator in (2) [see also (6)]. Physically, $\hat{q}$ characterizes the average squared transverse momentum transferred from the medium to a hard gluon per unit path length. Remarkably, for a static medium without time evolution, the small-distance properties of the Wilson line average (6) can be shown to determine the main properties of the medium-induced gluon radiation spectrum. Momentum broadening is characterized by $\langle k_\perp^2 \rangle \sim \hat{q} L_{\rm med}$ [4], the energy distribution is determined by the characteristic energy scale $\omega_c = \frac{1}{2} \hat{q} L_{\rm med}^2$ [4],

and medium effects regulate the additional gluon radiation in the infrared on a scale $\omega \sim \omega_c / \left(\hat{q} L^3_{\rm med}\right)^{2/3}$ [37]. For an expanding medium, the transport coefficient decreases with time - this translates into a path dependence $\hat{q} = \hat{q}(\xi)$ [38,13,39]. One finds, however, that the medium-induced gluon radiation spectrum for a dynamically expanding case is the same as that obtained for a static medium of rescaled linear line-averaged transport coefficient [39]

$$\bar{\hat{q}} = \frac{2}{L^2_{\rm med}} \int_0^{L_{\rm med}} \tau\, \hat{q}(\tau)\, d\tau\,. \qquad (9)$$

In practice, this dynamical scaling law allows a simplified data analysis in terms of static medium properties; a posteriori, one then translates the extracted static average transport coefficient into the realistic dynamical one. In what follows, we often denote the time-averaged transport coefficient by $\hat{q}$.

3 Leading hadron spectra

Up until now, experimental information about parton energy loss comes mainly from the study of single inclusive hadron spectra at high transverse momentum. How do we quantify "high" ? A qualitative assumption of the current picture of parton energy loss is that high-p_T partons are sufficiently Lorentz boosted to hadronize at large length scales (late times) outside the medium [25]. As a consequence, parton energy loss affects the *ratio* of identified hadron spectra at high p_T only to the extent to which the parent partons suffer different energy loss effects. Thus, parton energy loss can be the dominant medium effect only for $p_T > 6$ GeV, above the kinematical region in which the baryon-to-meson ratio shows an anomalous enhancement.

The transverse momentum of the leading hadron traces the energy of the leading parton in the parton shower and thus contains information about parton energy loss. However, the measurement of high-p_T hadrons induces a significant bias on the partonic fragmentation. For example, in a light quark jet, the leading hadronic fragment carries on average $\sim 1/4$ of the total jet energy, but a typical hadron in the high-p_T tail of a single inclusive spectrum carries typically $\sim 3/4$ of the energy of its parent parton. In the presence of a medium, this so-called trigger bias effect is medium-dependent: the parton which contributes to the high-p_T tail of the hadronic spectrum belongs to a fragmentation pattern which is much harder than the average, and thus it has an in-medium path length which is significantly smaller than the average. Also, for any given path length, it has a medium-induced energy loss which is smaller than the average. This explains why the notion of *average* parton energy loss is not suitable for calculating high-p_T hadron suppression [40]. What is needed in practice is the distribution in probability that a part ΔE of the total parton energy is radiated away. For the case of radiation of an arbitrary number of n *independent* gluon emissions, this probability reads [40,37]

$$P(\Delta E, L, \hat{q}) = \sum_{n=0}^{\infty} \frac{1}{n!} \left[\prod_{i=1}^{n} \int d\omega_i \frac{dI(\omega_i)}{d\omega}\right] \times \delta\left(\Delta E - \sum_{i=1}^{n} \omega_i\right) \exp\left[-\int_0^{\infty} d\omega \frac{dI}{d\omega}\right]. \qquad (10)$$

To model the effects of parton energy loss, the quenching weights $\mathcal{P}$ are convoluted with hard partonic cross sections and the parton fragmentation functions [12]. Since $\mathcal{P}$ is a probability distribution, this accounts for the above-mentioned trigger bias effects [37,40].

3.1 Determining the BDMPS transport coefficient $\hat{q}$ from R_{AA} for light-flavored hadrons

The medium-induced suppression of single inclusive hadron spectra $d^2N^{AA}/dp_T dy$ in nucleus-nucleus (AA) collisions is commonly quantified in terms of the nuclear modification factor

$$R_{AA}(p_T, y) = \frac{d^2N^{AA}/dp_T dy}{\langle T_{AA}\rangle_c d^2\sigma^{NN}/dp_T dy}\,. \qquad (11)$$

Here, $\langle T_{AA}\rangle_c$ is the standard nuclear overlap function, calculated as the average in the measured centrality class. In the absence of nuclear or medium effects, $R_{AA} \equiv 1$. We have calculated this factor for realistic nuclear geometry as described above [12]: For the hadron yield in AA collisions, nuclear modifications of the parton distribution functions [41] and parton energy loss was taken into account. The reference yield for nucleon-nucleon collisions is calculated in the same formalism without these medium effects. In the absence of parton energy loss, R_{AA} reduces slightly with increasing p_T since the relevant values of Bjorken x move from the anti-shadowing to the so-called EMC region where nuclear parton distribution functions decrease faster than proton ones with increasing x [42]. However, these pdf effects cannot account for the strength of the suppression. In contrast, final state parton energy loss can account for the degree of suppression.

Two features are remarkable [12]: First, the calculation indicates an approximately p_T-independent suppression pattern. The reason is that the slope of the partonic p_T-spectrum increases at RHIC gradually with increasing p_T. This is a trigger bias, according to which for the same value of R_{AA}, partons at higher p_T have to lose a smaller fraction of their total energy. Indeed, close to the kinematical boundary $p_T \sim O(\sqrt{s}/2$, for $p_T > 20 - 25$ GeV, the partonic spectrum at RHIC does not follow a power law but it has an approximately exponential shape. In this limit, the p_T-independence of R_{AA} is obvious, since

$$R_{AA} = \frac{\int d\Delta E\, \mathcal{P}(\Delta E)\, \exp\left[-(p_T + \Delta E)/E_{\rm slope}\right]}{\exp\left[-(p_T)/E_{\rm slope}\right]}\,. \qquad (12)$$

Secondly, Fig. 1 indicates that the absolute size of the suppression $R_{AuAu} \sim 0.2$ does not require a fine tuning of parameters but appears naturally from the interplay of parton energy loss and nuclear geometry. Indeed, as long as

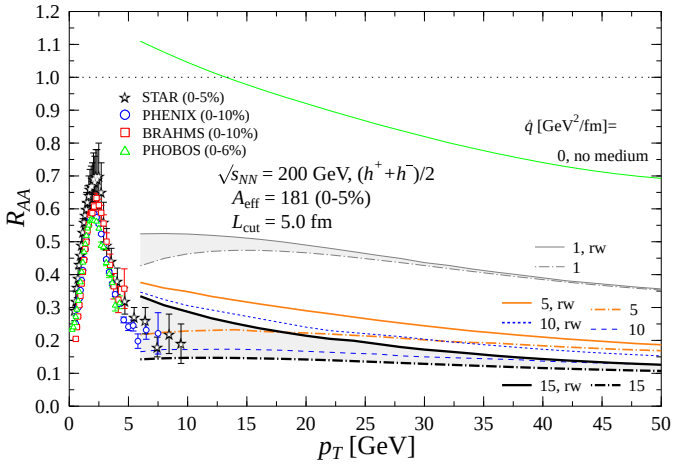

Fig. 1. The nuclear modification factor R_{AA} for charged hadrons in the 0-5 % most central Au+Au collisions at $\sqrt{s_{NN}}$ = 200 GeV for different values of the time-averaged transport coefficient $\hat{q}$. Differences between solid and dash-dotted curves indicate uncertainties related to finite energy corrections. Figure taken from [12].

the density of the medium is sufficiently high (i.e. $\hat{q}$ is large enough), R_{AuAu} approaches a factor 5 suppression for central collisions. However, even if one increases the density further, the suppression increases only slightly, since an essentially fixed fraction of the hard partons is produced in the outer corona of the two-dimensional transverse overlap of the nucleus-nucleus collision and thus remains almost unaffected due to a negligible in-medium path-length [43, 11,12]. This also implies that the sensitivity of single inclusive spectra to properties of the medium is rather limited: they provide only a lower bound on the produced density.

The model discussed above also accounts for the observed centrality dependence of the nuclear modification factor [10,44,11]. However, information about the centrality dependence does not appear to increase the sensitivity to properties of the medium. In fact, on the basis of the measured centrality dependence, one cannot even discriminate between a linear and a quadratic dependences of parton energy loss on $L_{\rm med}$ [14].

3.2 Dependence of parton energy loss on parton identity

The calculation of medium-induced gluon radiation predicts a hierarchy of parton energy loss depending on parton identity,

$$\Delta E_{\rm gluon} > \Delta E_{\rm quark,\, m=0} > \Delta E_{\rm quark,\, m\neq 0}\,. \qquad (13)$$

Gluons lose more energy than quarks due to their stronger coupling to the medium (*color charge effect*), and massive quarks lose even less energy than massless ones due to the mass-dependent phase-space restrictions on the medium-induced gluon radiation spectrum (*mass effect*) [45,46,47, 48]. Testing the hierarchy (13) is an important step towards verifying the microscopic partonic dynamics conjectured to underly high-p_T hadron suppression.

On the level of single inclusive spectra, one can test (13) by comparing the suppression of identified hadron spectra which differ in their parent partons. Of particular interest is the ratio of nuclear modification factors of high-p_T heavy-flavored mesons to light-flavored hadrons ("heavy-to-light ratio") [49]. In general, these ratios are sensitive to the color charge and the mass effect, but their sensitivity to both effects differs with center of mass energy, transverse momentum range and hadron identity. In Fig. 2, results are shown for the heavy-to-light ratios of D and B mesons at the LHC. For D meson spectra at high but experimentally accessible transverse momentum ($10 \sim p_T \sim 20$ GeV) in Pb–Pb collisions at the LHC, one finds that charm quarks behave essentially like light quarks. However, since light-flavored hadron yields are dominated by gluon parents, the heavy-to-light ratio of D mesons is a sensitive probe of the color charge dependence of parton energy loss. In contrast, due to the larger b quark mass, the medium modification of B mesons in the same kinematical regime provides a sensitive test of the mass dependence of parton energy loss. Hence, a combined analysis of D and B meson spectra at LHC will allow to clarify the parton species dependence of parton energy loss. At RHIC energies, the strategies for identifying and disentangling the color charge and mass dependence of parton energy loss are more involved. First, high-p_T hadron spectra test parton distribution functions at ~ 30 times higher Bjorken x than at the LHC. This implies that light-flavored hadrons have a more significant contribution of parent quarks, and heavy-to-light ratios are thus less sensitive to the color charge effect. Second, the kinematical regime suited for a characterization of the mass effect in with D meson spectra at RHIC is limited to $7 \sim p_T \sim 12$ GeV. On the other hand, in heavy-to-light ratios, color charge and mass effect do not compensate each other but lead both to an enhancement. So, even if it should be difficult to disentangle both effects, their combined contribution can be expected to leave a valuable additional information about parton energy loss.

Particle correlations may provide important complementary information for elucidating the influence of parton identity on final state parton energy loss. For example, requiring that a high-p_T trigger hadron at forward rapidity is balanced by a recoil at mid-rapidity, one may be able to study medium-modified hadron production in a configuration which enriches the contribution of gluon parents. Both at RHIC and at the LHC, the class of correlation measurements with this potential is large. It is an open question whether some of these measurements have a similar or even higher sensitivity to the mass and color charge dependence of parton energy loss than the ratios of particle identified single inclusive hadron spectra discussed above.

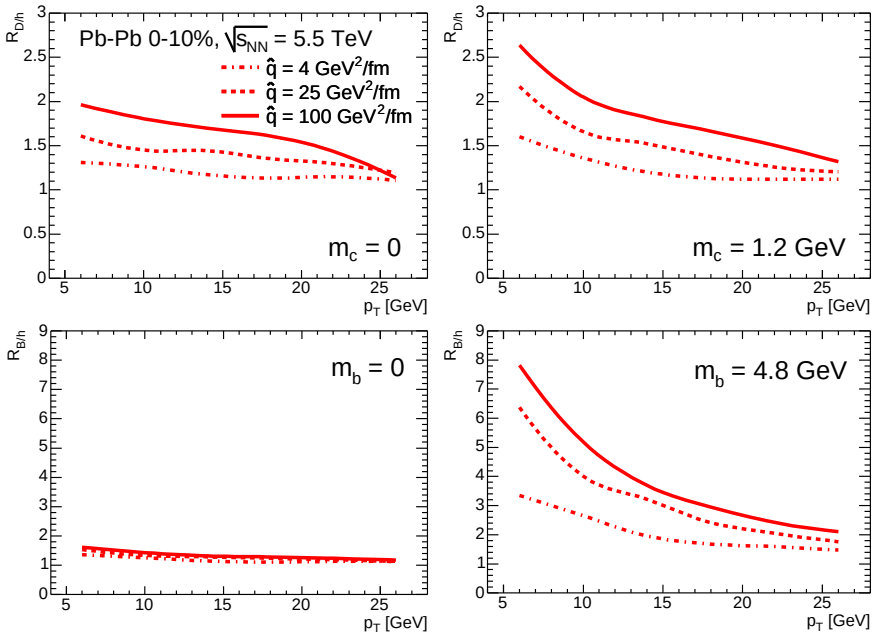

Fig. 2. Heavy-to-light ratios for D mesons (upper plots) and B mesons (lower plots) for the case of a realistic heavy quark mass (plots on the right) and for a case study in which the quark mass dependence of parton energy loss is neglected (plots on the left). Figure taken from [49].

3.3 What do we learn from R_{AA} about the medium ?

The first answer to this question is a number: the experimentally favored value of the time-averaged transport coefficient, $\overline{\hat{q}} \simeq 10\ \mathrm{GeV}^2/\mathrm{fm}$. Formally, this quantity characterizes the small-distance property of the expectation value (2) of two light-like Wilson lines in the target average characterizing the produced medium. The main question is whether this value for $\overline{\hat{q}}$ is consistent with expectations for a thermalized system. For this problem, standard lattice techniques do not apply, and it is an open challenge of how to perform the calculation of the average (2) in a thermal heat bath. Novel approaches are clearly needed, and may involve new concepts such as exploiting AdS/CFT correspondence [50]. On a less ambitious level, even if the initial conditions of (2) cannot be calculated, the energy dependence of (2) should be predictable since it is expected to satisfy non-linear small-x evolution equations.

The only attempt so far to calculate the transport coefficient $\overline{\hat{q}}$ for a QCD equilibrium state is rather model dependent [51] [for another recent discussion, see also Ref. [52] in these proceedings]. In general, $\hat{q}$ is expected to be proportional to the number density of scattering centers, and hence for an ideal gas

$$\hat{q}(\tau) = c\,\epsilon^{3/4}(\tau)\,. \tag{14}$$

Here, c is a medium-dependent proportionality constant. To determine it for a quark gluon plasma, Ref. [51] estimates the momentum transfer from the medium to the hard parton per medium constituent by modeling these constituents with temperature dependent Debye-screened scattering potentials. One finds [51]

$$c_{\mathrm{QGP}}^{\mathrm{ideal}} \approx 2\,. \tag{15}$$

This estimate is based on the strong assumptions spelled out above; clearly, an alternative calculation would be desirable. Here, we explore the consequences if the number (15) is taken seriously.

For an expanding medium with expansion parameter α, and $\hat{q}(\tau) = \hat{q}(\tau_0)\ (\tau_0/L)^\alpha$, one finds from the dynamical scaling law (9)

$$c = \frac{\hat{q}(\tau_0)}{\epsilon(\tau_0)^{3/4}} = \frac{\overline{\hat{q}}}{\epsilon(\tau_0)^{3/4}} \frac{2-\alpha}{2} \left(\frac{L}{\tau_0}\right)^\alpha . \tag{16}$$

For a typical initial time $\tau_0 \sim 0.2$ fm/c, the average in-medium pathlength may be as small as $L \sim 10\,\tau_0 = 2$ fm . The energy density averaged over a uniform transverse profile at initial time τ_0 can be as large as $\epsilon(\tau_0) \sim O(100)\frac{\mathrm{GeV}}{\mathrm{fm}^3}$ [53], although much smaller estimates exist [54] This implies that realistic scenarios lie in the parameter range $\epsilon(\tau_0) < 100\,\frac{\mathrm{GeV}}{\mathrm{fm}^3}$, $L \sim 10\,\tau_0$, $0.75 < \alpha < 1.5$, for which one finds

$$c > 8 \ldots 19 > (4-5)\, c_{\mathrm{QGP}}^{\mathrm{ideal}}\,. \tag{17}$$

Taken at face value, this number quantifies the extent to which the produced medium deviates from an ideal quark gluon plasma. Interactions between the medium and the hard partonic test particle are at least a factor $\sim 4-5$ stronger than perturbatively expected. Remarkably, to reproduce an elliptic flow in agreement with experiment, parton cascade calculations require partonic

cross sections which are a similar factor $\sim 4-5$ larger than perturbatively expected [55]. This supports the picture that hard partons are *test particles* which participate in the same equilibration processes as bulk degrees of freedom. It strengthens the motivation that the analysis of medium-modified hard parton fragmentation provides access to QCD equilibration dynamics. This leads us to several far-reaching questions all of which require a better dynamical understanding of the transport coefficient $\hat{q}$. For example: Is an interaction strength of the size (17) compatible with the known residual interactions in a QGP which result in a $\sim 20\%$ deviation of the energy density from the ideal Stefan-Boltzmann limit at high temperature ?

4 Medium-modification of jets

We have argued above hat the study of medium modified parton fragmentation provides access to partonic thermalization processes. The remnants of a hard parton are thermalized to the extent to which they cannot be distinguished any more from the typical degrees of freedom in the approximate heat bath provided by the medium. Leading hadrons provide only partial and highly biased information about the medium-dependent dynamics which drives partonic fragmentation towards thermal equilibrium. There is an obvious danger that e.g. leading high-p_T trigger particles bias the fragmentation such that information about the thermal properties of the *average* partonic fragmentation is lost. The need to study the unbiased average parton fragmentation pattern provides a strong motivation to go beyond single inclusive hadron spectra and to analyze the medium-modification of internal jet properties. Other motivations come from arguments that internal jet structures are more sensitive to properties of the medium [28] and that they allow us to disentangle different characteristic properties of the medium (such as strength of collective motion and local density [30,31]) which are difficult to disentangle with single inclusive spectra alone.

4.1 Broadening of jet energy and multiplicity distributions

As discussed in section 2, theory predicts a one-to-one correspondence between the energy degradation of the leading parton (governed by the characteristic gluon energy $\omega_c = \frac{1}{2}\hat{q}L^2$) and the transverse-momentum broadening of the parton shower [36,37] (governed by $\hat{q}L$). To go beyond leading hadron spectra, one can study jet-like near-side particle correlations associated to high-p_T trigger particles [29,26], particle distributions associated to trigger particles, or calorimetrically reconstructed "true" jets measurements [28,30]. One possibility to characterize the transverse phase space distribution of a jet is by measuring the fraction $\rho(R)$ of the total jet energy E_t deposited within a subcone of radius $R = \sqrt{(\Delta\eta)^2 + (\Delta\Phi)^2}$,

$$\rho_{\rm vac}(R) = \frac{1}{N_{\rm jets}} \sum_{\rm jets} \frac{E_t(R)}{E_t(R=1)} \,. \qquad (18)$$

Such measurements have been performed e.g. by the D0 collaboration [56]. If the BDMPS transport coefficient is very large, an experimentally accessible broadening of this jet shape may be expected. However, for $\hat{q} = 1{\rm GeV}^2/fm$, it was found that the broadening of an $E_T = 100$ GeV jet is negligible [28]. In this case, the average jet energy fraction inside a small jet cone $R = 0.3$ was reduced by ~ 3 % only. This should be compared to estimates of the background energy $E_t^{\rm bg}$ deposited inside the same jet cone which for an event multiplicity $dN^{\rm ch}/dy = 2500$ at LHC is of roughly the same size, $E_t^{\rm bg} \sim 100$ GeV. The example indicates that transverse jet energy distributions, even if deviations from the vacuum jet shapes can be detected, may be of limited sensitivity for a detailed characterization of the medium. The physics reason is that the most energetic jet fragments, which dominate measures of the type (18), are almost collinear and change their angular orientation very little by medium-induced scattering.

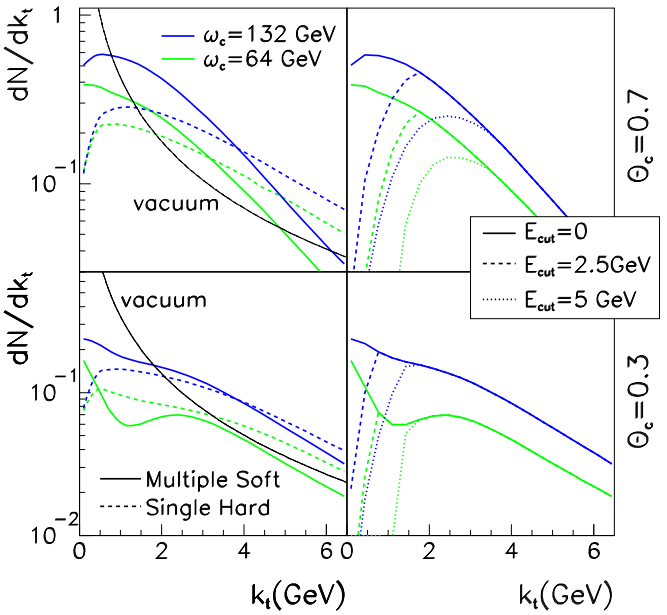

Fig. 3. The gluon multiplicity distribution inside a jet cone size $R = \Theta_c$, measured as a function of k_t with respect to the jet axis. Removing gluons with energy smaller than $E_{\rm cut}$ from the distribution (dashed and dotted lines) does not affect the high-k_t tails. Figure taken from [28].

If medium effects do not change the jet energy distribution significantly while the energy of leading hadrons decreases strongly, then a significant change in the jet multiplicity distributions is unavoidable. It is of particular interest to identify those multiplicity measurements which are almost insensitive to the high multiplicity background in nucleus-nucleus collsions. In Fig. 3, we show the medium-induced additional number of gluons with transverse momentum $k_t = |\mathbf{k}|$, produced within a subcone of opening angle θ_c, as calculated from (7), see [28]. This distribution is compared to the approximate shape of the corresponding distribution in the vacuum.The total par-

tonic jet multiplicity is the sum of both components. For realistic values of medium density and in-medium pathlength, medium effects are seen to increase this multiplicity significantly (by a factor > 2) in particular in the high-k_t tails. Also, the shape and width of the distribution changes sensitively with the scattering properties of the medium. Moreover, since gluons must have a minimal energy $\omega > k_t/\sin\Theta_c$ to be emitted inside the jet cone, this high-k_t tail is unaffected by "background" cuts on the soft part of the spectrum, see Fig. 3. The insensitivity of the high-k_t tail to the low E_t background and its sensitivity to the transverse momentum picked up from the medium are both based on kinematic grounds and should not depend on the details of our calculation. Thus, the qualitative conclusions drawn from this study are expected to remain unaffected by the uncertainties of our calculation and the effects of subsequent hadronization. On general grounds, jet multiplicity distributions appear to be more sensitive to medium properties than jet energy distributions.

4.2 Interplay of jet quenching and collective flow

To what extent do jet observables allow us to characterize qualitatively novel properties of the produced dense QCD matter which cannot be accessed with leading hadron spectra ? The general answer to this question is not known, but first model calculations indicate that novel information becomes indeed accessible:

One open issue is that parton energy loss is currently characterized in terms of the BDMPS transport coefficient which, according to (14), characterizes the local particle density of the produced matter. On the other hand, there is strong experimental evidence that the produced medium is - if at all - only *locally* equilibrated and is thus characterized only *locally* by its energy density. Measurements of low-p_T inclusive hadron spectra [57,58] and their azimuthal asymmetry [59,60,61] support the picture that different hadron species emerge from a common medium which has built up a strong collective velocity field [62]. These measurements are broadly consistent with calculations based on ideal hydrodynamics [62], in which the dynamic behavior of the produced QCD matter is fully specified by its equation of state $p = p(\epsilon, T, \mu_B)$ which enters the energy momentum tensor

$$T^{\mu\nu}(x) = (\epsilon + p)\, u^\mu\, u^\nu \, - p\, g^{\mu\nu}\,. \qquad (19)$$

Shouldn't parton energy loss be sensitive to $T^{\mu\nu}(x)$ and thus to a combination of particle density and flow effects ? To quantify the effect of collective flow on parton fragmentation, we have extended the formalism of medium-induced parton energy loss (7) to the case of flow-induced azimuthally oriented momentum transfer [30,31]. One finds that flow effects generically result in characteristic asymmetries in the $\eta \times \phi$-plane of jet energy distributions and of multiplicity distributions associated to high-p_T trigger particles, see Fig. 4. First experimental

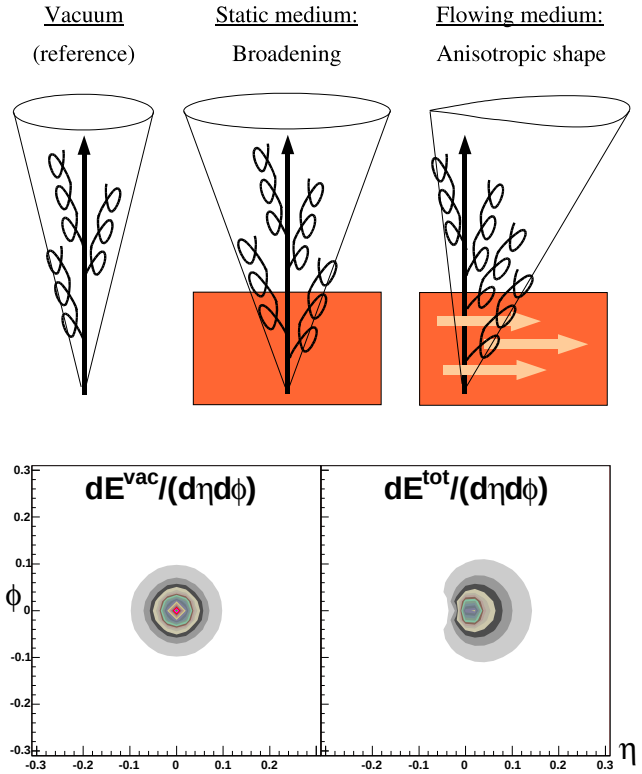

Fig. 4. Upper part: sketch of the distortion of the jet energy distribution in the presence of a medium with or without collective flow. Lower part: calculated distortion of the jet energy distribution in the $\eta \times \phi$-plane for a 100 GeV jet. The right hand-side is for an average medium-induced radiated energy of 23 GeV and equal contributions from density and flow effects. Figures taken from [30].

support for this picture comes from the enhanced and broadened rapidity distribution of hadron production associated to trigger particles [63,30]. Flow effects on the associated initial state radiation may also play a role in accounting for these data [64]. Moreover, model calculations indicate that collective flow also contributes to the medium-induced suppression of single inclusive high-p_T hadron spectra. In particular, one finds that low-p_T elliptic flow can induce a sizeable additional contribution to the high-p_T azimuthal asymmetry by selective elimination of those hard partons which propagate with significant inclination against the flow field [31]. This reduces at least partially the problem that models of parton energy loss tend to underpredict the large azimuthal asymmetry v_2 of high-p_T hadronic spectra in semi-peripheral Au+Au collisions [14,11]. This is a first example of how a detailed dynamical characterization of the internal jet structure may give access to qualitatively novel information about the collective properties of the produced matter. Another recent suggestion is based on the observation that in an ideal fluid, energy can be radiated only by sound waves. This could lead to the dramatic phenomenon that hadron production associated to high-p_T trigger particles emerges like a sonic boom preferentially under angles characteristic of the sound velocity of the produced medium [65].

In conclusion, the study of jet-like particle correlations and jet measurements in heavy ion collisions is still at the very beginning. There are strong motivations to expect that analyzing the interplay of parton fragmentation and medium properties will provide a laboratory for QCD equilibrium and non-equilibrium physics which is of unmatched versatility and accuracy.

I thank Nestor Armesto, Andrea Dainese, Alex Kovner and Carlos Salgado for the work done together. I am particularly grateful to Peter Jacobs for many discussions and helpful comments about this manuscript.

References

1. R. Baier, D. Schiff and B. G. Zakharov, Ann. Rev. Nucl. Part. Sci. **50**, 37 (2000) [arXiv:hep-ph/0002198].
2. A. Kovner and U. A. Wiedemann, arXiv:hep-ph/0304151.
3. M. Gyulassy, I. Vitev, X. N. Wang and B. W. Zhang, arXiv:nucl-th/0302077.
4. R. Baier, Y. L. Dokshitzer, A. H. Mueller, S. Peigne and D. Schiff, Nucl. Phys. B **484** (1997) 265.
5. B. G. Zakharov, JETP Lett. **65** (1997) 615.
6. U. A. Wiedemann, Nucl. Phys. B **588** (2000) 303.
7. M. Gyulassy, P. Levai and I. Vitev, Nucl. Phys. B **594** (2001) 371.
8. X. N. Wang and X. f. Guo, Nucl. Phys. A **696** (2001) 788.
9. M. H. Thoma, arXiv:hep-ph/9503400.
10. X. N. Wang, Phys. Lett. B **579** (2004) 299.
11. A. Dainese, C. Loizides and G. Paic, Eur. Phys. J. C **38** (2005) 461.
12. K. J. Eskola, H. Honkanen, C. A. Salgado and U. A. Wiedemann, Nucl. Phys. A **747** (2005) 511.
13. M. Gyulassy, I. Vitev and X. N. Wang, Phys. Rev. Lett. **86** (2001) 2537.
14. A. Drees, H. Feng and J. Jia, arXiv:nucl-th/0310044.
15. I. Vitev and M. Gyulassy, Phys. Rev. Lett. **89** (2002) 252301.
16. T. Hirano and Y. Nara, Phys. Rev. C **66** (2002) 041901.
17. K. Adcox *et al.* [PHENIX Collaboration], Phys. Rev. Lett. **88** (2002) 022301.
18. S. S. Adler *et al.* [PHENIX Collaboration], Phys. Rev. C **69** (2004) 034910.
19. C. Adler *et al.* [STAR Collaboration], Phys. Rev. Lett. **89** (2002) 202301.
20. J. Adams *et al.* [STAR Collaboration], Phys. Rev. Lett. **91** (2003) 172302.
21. B. B. Back *et al.* [PHOBOS Collaboration], Phys. Lett. B **578** (2004) 297.
22. I. Arsene *et al.* [BRAHMS Collaboration], Phys. Rev. Lett. **91** (2003) 072305.
23. C. Adler *et al.* [STAR Collaboration], Phys. Rev. Lett. **90** (2003) 082302.
24. J. Adams *et al.* [STAR Collaboration], Phys. Rev. Lett. **93**, 252301 (2004).
25. U. A. Wiedemann, J. Phys. G **30** (2004) S649.
26. A. Majumder and X. N. Wang, Phys. Rev. D **70** (2004) 014007.
27. A. Majumder, E. Wang and X. N. Wang, arXiv:nucl-th/0412061.
28. C. A. Salgado and U. A. Wiedemann, Phys. Rev. Lett. **93**, 042301 (2004).
29. S. Pal and S. Pratt, Phys. Lett. B **574** (2003) 21.
30. N. Armesto, C. A. Salgado and U. A. Wiedemann, Phys. Rev. Lett. **93** (2004) 242301.
31. N. Armesto, C. A. Salgado and U. A. Wiedemann, arXiv:hep-ph/0411341.
32. W. Buchmuller and A. Hebecker, Nucl. Phys. B **476** (1996) 203.
33. U. A. Wiedemann, Nucl. Phys. B **582**, 409 (2000).
34. A. Kovner and U. A. Wiedemann, Phys. Rev. D **64**, 114002 (2001).
35. Y. V. Kovchegov and A. H. Mueller, Nucl. Phys. B **529** (1998) 451.
36. U. A. Wiedemann, Nucl. Phys. A **690** (2001) 731.
37. C. A. Salgado and U. A. Wiedemann, Phys. Rev. D **68** (2003) 014008.
38. R. Baier, Y. L. Dokshitzer, A. H. Mueller and D. Schiff, Phys. Rev. C **58** (1998) 1706.
39. C. A. Salgado and U. A. Wiedemann, Phys. Rev. Lett. **89** (2002) 092303.
40. R. Baier, Y. L. Dokshitzer, A. H. Mueller and D. Schiff, JHEP **0109** (2001) 033.
41. K. J. Eskola, V. J. Kolhinen and C. A. Salgado, Eur. Phys. J. C **9** (1999) 61.
42. K. J. Eskola and H. Honkanen, Nucl. Phys. A **713** (2003) 167.
43. B. Muller, Phys. Rev. C **67** (2003) 061901.
44. X. N. Wang, Phys. Lett. B **595**, 165 (2004).
45. Y. L. Dokshitzer and D. E. Kharzeev, Phys. Lett. B **519** (2001) 199.
46. N. Armesto, C. A. Salgado and U. A. Wiedemann, Phys. Rev. D **69** (2004) 114003.
47. M. Djordjevic and M. Gyulassy, Nucl. Phys. A **733**, 265 (2004).
48. B. W. Zhang, E. Wang and X. N. Wang, arXiv:nucl-th/0309040.
49. N. Armesto, A. Dainese, C. A. Salgado and U. A. Wiedemann, arXiv:hep-ph/0501225.
50. S. J. Sin and I. Zahed, arXiv:hep-th/0407215.
51. R. Baier, Nucl. Phys. A **715** (2003) 209.
52. B. Muller and K. Rajagopal, arXiv:hep-ph/0502174.
53. K. J. Eskola, K. Kajantie, P. V. Ruuskanen and K. Tuominen, Nucl. Phys. B **570** (2000) 379.
54. N. Armesto, C. A. Salgado and U. A. Wiedemann, Phys. Rev. Lett. **94** (2005) 022002.
55. D. Molnar and M. Gyulassy, Nucl. Phys. A **697** (2002) 495 [Erratum-ibid. A **703** (2002) 893].
56. B. Abbott, M. Bhattacharjee, D. Elvira, F. Nang and H. Weerts [D0 Coll.], FERMILAB-PUB-97-242-E
57. S. S. Adler *et al.* [PHENIX Collaboration], Phys. Rev. C **69** (2004) 034909.
58. J. Adams *et al.* [STAR Collaboration], Phys. Rev. Lett. **92** (2004) 112301.
59. K. H. Ackermann *et al.* [STAR Collaboration], Phys. Rev. Lett. **86** (2001) 402.
60. K. Adcox *et al.* [PHENIX Collaboration], Phys. Rev. Lett. **89** (2002) 212301.
61. S. S. Adler *et al.* [PHENIX Collaboration], Phys. Rev. Lett. **91** (2003) 182301.
62. P. F. Kolb and U. Heinz, arXiv:nucl-th/0305084.
63. F. Wang [STAR Collaboration], arXiv:nucl-ex/0404010; D. Magestro in these proceedings.
64. S. A. Voloshin, arXiv:nucl-th/0312065.
65. J. Casalderrey-Solana, E. V. Shuryak and D. Teaney, arXiv:hep-ph/0411315.